Phys Chem Minerals (2000) 27: 533–544

ORIGINAL PAPER

E. Ohtani · H. Mizobata · H. Yurimoto

Stability of dense hydrous magnesium silicate phases in the systems Mg_2SiO_4-H_2O and $MgSiO_3$-H_2O at pressures up to 27 GPa

Received: 4 August 1999 / Accepted: 1 March 2000

Abstract We conducted high-pressure phase equilibrium experiments in the systems $MgSiO_3$ with 15 wt% H_2O and Mg_2SiO_4 with 5 wt% and 11 wt% H_2O at $20 \sim 27$ GPa. Based on the phase relations in these systems, together with the previous works on the related systems, we have clarified the stability relations of dense hydrous magnesium silicates in the system MgO-SiO_2-H_2O in the pressure range from 10 to 27 GPa. The results show that the stability field of phase G, which is identical to phase D and phase F, expands with increasing water contents. Water stored in serpentine in the descending cold slabs is transported into depths greater than 200 km, where serpentine decomposes to a mixture of phase A, enstatite, and fluid. Reaction sequences of the hydrous phases which appear at higher pressures vary with water content. In the slabs with a water content less than about 2 wt%, phase A carries water to a depth of 450 km. Hydrous wadsleyite, hydrous ringwoodite, and ilmenite are the main water reservoirs in the transition zone from 450 to 660 km. Superhydrous phase B is the water reservoir in the uppermost part of the lower mantle from 670 to 800 km, whereas phase G appears in the lower mantle only at depths greater than 800 km. In cold slabs with local water enrichment greater than 2 wt%, the following hydrous phases appear with increasing depths; phase A to 450 km, phase A and phase G from 450 km to 550 km, brucite, superhydrous phase B, and phase G from 550 km to 800 km, and phase G at depths greater than 800 km.

Key words High pressure, High temperature · DHMS · phases A–G

E. Ohtani (✉) · H. Mizobata
Institute of Mineralogy, Petrology, and Economic Geology, Tohoku University, Sendai 980-8578, Japan
Tel. 81-22-217-6662, Fax: 81-22-217-6675
e-mail: ohtani@mail.cc.tohoku.ac.jp

H. Yurimoto
Tokyo Institute of Technology, Meguro-ku, Tokyo 152, Japan

Introduction

Water plays important roles in the Earth's interior, i.e., it promotes magma generation and phase transformation kinetics, and affects the mantle dynamics by softening the mantle minerals (e.g., Kubo et al. 1998). Therefore, it is essential to clarify the state of water in the Earth's interior.

Various dense hydrous magnesium silicates (DHMS) have been synthesized to date in the system of MgO-SiO_2-H_2O (e.g., Ringwood and Major 1967; Liu 1987; Gasparik 1990; Kanzaki 1991), and these phases are expected to exist in the cold subducting slabs descending into the lower mantle. DHMS phases, hydrous wadsleyite, and hydrous ringwoodite (e.g., Inoue et al. 1995) are the candidates for water reservoirs in the mantle. However, detailed phase relations of these hydrous silicate phases at high pressures in the Earth's interior are still a matter of great debate. The chemical compositions of DHMS phases discussed in this paper are summarized in Fig. 1.

The purpose of this work is to conduct high-pressure phase equilibrium experiments in the systems Mg_2SiO_4-H_2O and $MgSiO_3$-H_2O at pressures up to 27 GPa and to evaluate the possibility of water reservoirs and water transportation into the deep mantle by subduction processes.

Experimental

Sample preparation

Several starting materials with the bulk compositions of Mg_2SiO_4 with 15 and 11 wt% H_2O and $MgSiO_3$ with 15 wt% H_2O were prepared as the mixtures of the reagents $Mg(OH)_2$, SiO_2 and synthesized forsterite Mg_2SiO_4 in appropriate proportions. Compositions of the starting materials are summarized in Fig. 2. The starting materials were stored in a vacuum desiccator to avoid formation of hydroxycarbonate $Mg(OH)_2MgCO_3$ by absorption of carbon dioxide. The sample was enclosed in a platinum capsule sealed by welding to protect from water loss during the run.

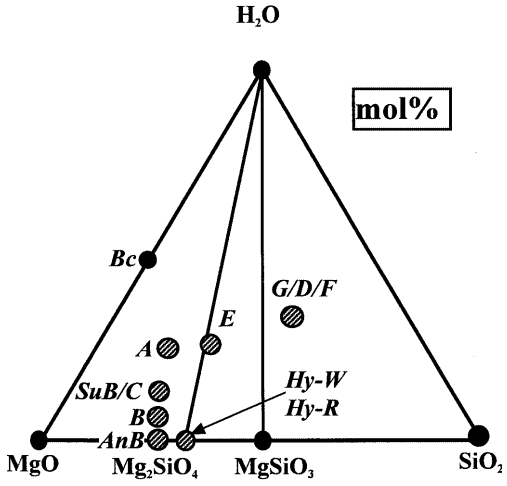

Fig. 1 Compositions of dense hydrous magnesium silicates (DHMS) phases in the MgO-SiO_2-H_2O system. *A* Phase A; *E* phase E; *SuB* superhydrous phase B; *G* phase G; *D* phase D by Yang et al. (1997); *F* phase F by Kanzaki (1991); *Hy-W* hydrous wadsleyite; *Hy-R* hydrous ringwoodite

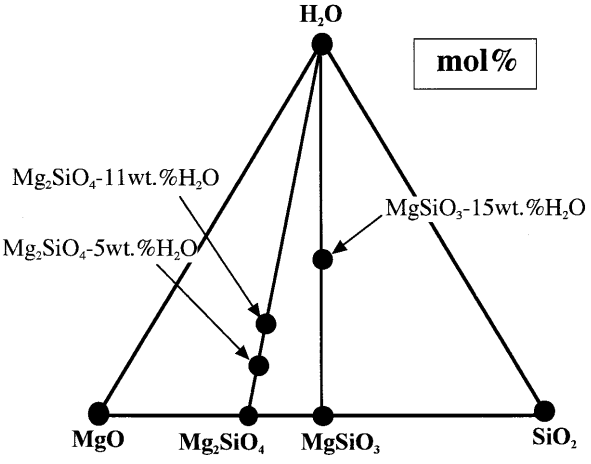

Fig. 2 Compositions of the starting materials; $MgSiO_3$-15 wt% H_2O, Mg_2SiO_4-5 wt% H_2O, and Mg_2SiO_4-11 wt% H_2O compositions

High-pressure and high-temperature experiments

High-pressure and high-temperature experiments were carried out using the Kawai anvil (MA8 type multianvil) driven by a 3000-ton uniaxial press with a DIA-type cubic guide block system at Tohoku University (Ohtani et al. 1998). The MA8-type multianvil is called here the Kawai anvil in honor of the pioneering work by Kawai (e.g., Kawai and Endoh 1970). Our DIA-type guide block has anvils with an edge length of 50 mm. The Kawai anvil used here is composed of eight tungsten carbide cubic anvils with a truncated edge length (TEL) of 2 mm. Preformed pyrophyllite gaskets were used between the cubes. Figure 3 shows a typical furnace assembly used for the anvils with 2-mm truncation. Semisintered zirconia (ZrO_2) octahedra were used as the pressure medium, and lanthanum chromite ($LaCrO_3$) tubes as the heating element. A magnesia sleeve was placed between the lanthanum chromite heater and the platinum capsule for electrical insulation. Pressure was calibrated on the basis of the phase boundaries of ilmenite-perovskite transition in $MgSiO_3$ (Kato et al. 1995) and the decomposition reaction of ringwoodite, Mg_2SiO_4, to perovskite, $MgSiO_3$, and periclase, MgO (Ito and Takahashi 1989), at 1600 °C. The pressure was increased to the desired value first and held constant, and then AC power was supplied to the lanthanum chromite tube heater in the furnace assembly. Temperature was measured with a W3%Re-W25%Re thermocouple 0.1 mm in diameter. The temperature difference within the capsule was less than 50 °C. After heating at high pressure, the charge was quenched by shutting off the electric power supply. The samples were recovered after releasing pressure slowly in 1 day.

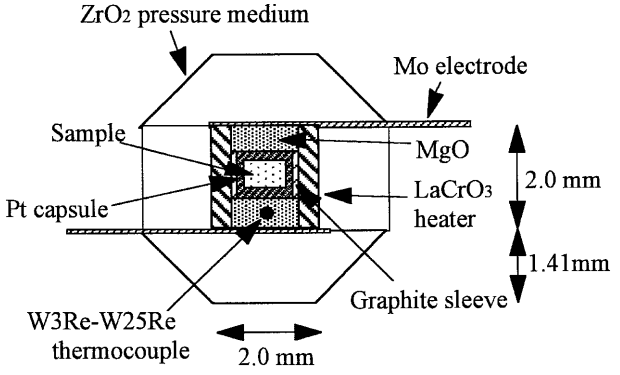

Fig. 3 The furnace assembly for the anvils with the truncated edge length of 2 mm

Characterization of run products

Recovered samples were mounted in epoxy resin and carefully polished for measuring the chemical composition using an electron probe microanalyzer (EPMA, JEOL JXL8800M). The operating conditions were 15 kV and 10 nA. The phases were identified by X-ray powder diffraction or micro-Raman spectroscopy. The X-ray powder diffraction was carried out by a Debye-Scherrer Camera with a Gandolfi attachment. A micro-area X-ray diffractometer (RINT 2000) was also used for analyzing the run products from some experiments. Raman spectra were measured using a micro-Raman spectrometer (JASCO NRS-2000). The Ar^+ laser with a wavelength of 514.5 nm and laser power of 30 mW was focused on an area of the sample about 1 μm in diameter.

Hydrogen in some hydrous phases was identified by micro-Raman and infrared (IR) spectroscopies. The IR spectra of some run products were measured using a micro-Fourier-transform infrared spectrometer (JEOL Diamond-20). The water contents in hydrous ringwoodite (Mg_2SiO_4) were measured by the secondary ion mass spectrometry (SIMS) using a Cameca IMS-3F ion microprobe at the Tokyo Institute of Technology. SIMS is an ideal tool for the determination of hydrogen contents in a micro-area of the sample (Yurimoto et al. 1989). A 10-nA and 10-kV $^{16}O^-$ primary beam was focused to a spot about 50 μm in diameter. Secondary $^1H^+$ and $^{30}Si^+$ ions were collected at the central region ($10 \sim 20$ μm in diameter) of the sputtered area using a mechanical aperture and analyzed by −100 V offsetting of the sample accelerating voltage. The energy slit was set to accept a 20-eV window, resulting in a mass resolution $M/\Delta M = \pm 500$. The pressure in the sample chamber was maintained below 0.5 μPa. The samples for SIMS measurements were coated by gold film on the surface in order to eliminate electrostatic charging. Other analytical and instrumental conditions were similar to previous studies (Kurosawa et al. 1992; Miyagi and Yurimoto 1995). For quantitative analysis, natural hornblende (Miyagi and Yurimoto 1995), San Carlos olivine (Kurosawa et al. 1992), and $MgSiO_3$ glass were used as standards.

Results

$MgSiO_3$-H_2O system

Experimental conditions and the results are summarized in Table 1. The backscattered electron images of

Table 1 Experimental conditions and results in the $MgSiO_3$-15 wt% H_2O bulk composition. *Il* Ilmenite; *Pv* perovskite; *Pc* periclase; *St* stishovite; *L* liquid; *G* phase G; *SuB* superhydrous phase B; *E* phase E; *Bc* brucite

Run no.	Pressure (GPa)	Temperature (°C)	Time (h)	Results
E15H09	20	880	12	G + SuB + L[b]
E15H04	20	1100	3	G + SuB + L[b]
EHF04[a]	20	1290	1	L + St + E
EH01[a]	22	1050	3	G + SuB + L[b]
E15H05	23	880	12.5	G + trace Bc + L
				G + Pv + trace Bc
E15H03	23	1100	3	G + SuB + L[b]
				G + SuB + Il/Pv
E15H08	23	1300	2	L + G + SuB
E15H06	25	880	12	G + trace Bc + L
				G + Pv + trace Bc
EH04[a]	25	1100	3	G + Pc + L[a]
E15H01	25	1150	5	G + SuB + L
				G + SuB + Pv
E15H02	25	1430	3.5	L + Pv + St

[a] The bulk composition is $MgSiO_3$-14 wt% H_2O containing 2.6 wt% CO_2
[b] Trace amount of magnesite was observed in the run products

the run products are given in Fig. 4. The phase relations in the $MgSiO_3$-15 wt% H_2O bulk composition are given in Fig. 5. The experiments were conducted at 20 to 25 GPa pressure and 850 to 1500 °C temperature. At lower temperatures around 850 °C, we observed the coexistence of phase G and brucite at around 23 ~ 25 GPa. Phase G coexists with superhydrous phase B at around 1100 °C in the same pressure range. The presence of fluid during the experiments was confirmed in some runs by the presence of fluid in the recovered capsule. Liquids in some runs were recovered as quench crystals with dendritic textures that are similar to the quench liquids observed in melting experiments under the dry condition. The quench liquids were highly magnesian in composition. The phases coexisting with liquids at 1300 °C were phase E, stishovite at 20 GPa, and phase G and superhydrous phase B at 23 GPa. The Mg/Si ratio of phase E determined by EPMA varies from 1.88 to 1.90. We observed the coexistence of liquid, $MgSiO_3$ perovskite, and stishovite at 25 GPa and 1500 °C in the $MgSiO_3$-15 wt% H_2O, suggesting that the liquid has a magnesium-rich composition.

We observed the assemblage of phase G + superhydrous phase B + perovskite/ilmenite in some runs at 25 GPa and 1150 °C, perhaps due to the temperature gradient and/or the difference in the water fugacity. A trace amount of magnesite was detected in some run products in this system; it was identified by using micro-Raman spectroscopy, perhaps due to absorption of a trace amount of carbon dioxide in air in spite of careful handling. Since magnesite was found only in trace amounts, we ignored it in the phase relations of the systems $MgSiO_3$-H_2O and Mg_2SiO_4-H_2O.

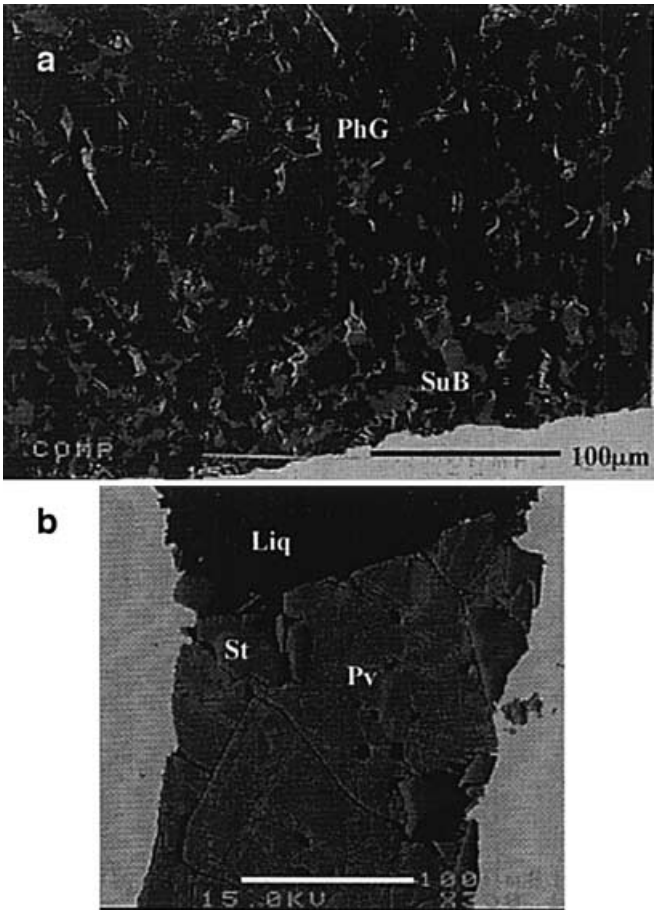

Fig. 4a, b Backscattered electron images (BEI) of the run products in the $MgSiO_3$-15 wt% H_2O system. **a** 25 GPa and 1150 °C (run E15H01). **b** 25 GPa and 1430 °C (run E15H02). *PhG* Phase G, *SuB* Superhydrous phase B, *St* stishovite, *Pv* perovskite, *Liq* liquid

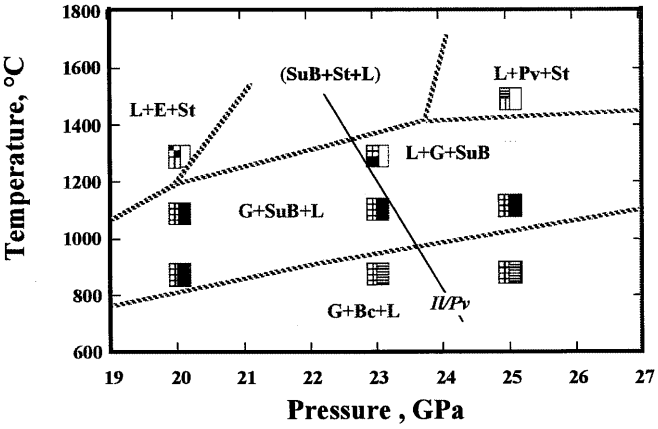

Fig. 5 Phase relation for the $MgSiO_3$-15 wt% H_2O bulk composition. *L* liquid; *E* phase E; *St* stishovite; *Pv* perovskite; *Il* ilmenite; *G* phase G, which is identical to phase D and phase F; *SuB* superhydrous phase B, which is identical to phase C; *Bc* brucite

Mg_2SiO_4-H_2O system

Experimental conditions and results in the system Mg_2SiO_4-H_2O containing 5 and 11 wt% H_2O are sum-

marized in Table 2 and are shown in Fig. 6a and b, respectively.

Mg_2SiO_4-5 wt% H_2O system

Figures 5 and 6a show that the stability field of phase G in this system is narrower than in the $MgSiO_3$-15 wt% H_2O system. Phase G appears in a limited pressure and temperature range above 23 GPa and below 1100 °C. Superhydrous phase B is stable in a wider pressure range from 20 to at least 25 GPa. Phase assemblages observed at 900 ~ 1100 °C with increasing pressure can be summarized as follows; superhydrous phase B + ilmenite + stishovite at 20 and 23 GPa, perovskite + superhydrous phase B + phase G at 25 GPa. Water partitioned into phase G relative to superhydrous phase B with increasing pressure, as will be discussed later. At temperatures higher than that of the stability limit of superhydrous phase B, phase assemblages such as ringwoodite + fluid, and the postspinel phases + fluid are observed.

The phase boundaries of ilmenite-perovskite transition and the decomposition reaction of ringwoodite into periclase and $MgSiO_3$ perovskite are also shown in Figs. 5 and 6. Superhydrous phase B and phase G could be stable in the cold slabs descending into the upper part of the lower mantle. In comparison to the phase boundaries of the $MgSiO_3$ ilmenite-perovskite transition and the decomposition of ringwoodite determined here under dry conditions, the present experiments suggest that the stability field of hydrous ringwoodite expands into higher pressure range by at least 0.5 GPa in the Mg_2SiO_4-5 wt% H_2O system, although more careful studies are needed to confirm this more quantitatively.

The assemblage ilmenite, superhydrous phase B, and stishovite transforms to peroviskite, superhydrous phase B, and phase G, as shown in Fig. 6a. Although the quantitative measurement of water in hydrous phases was not made by the present EPMA analysis, we may expect the following reaction; Mg_2SiO_4 + 0.39 H_2O (5 wt%) = 0.195SuB + 0.05Il + 0.365St = 0.44 Pv + 0.148SuB + 0.066G, of which reaction can be reduced to the following reaction, SuB + 7.8St = 8.3Pv + 1.4G, by presuming that the chemical compositions of observed phases are approximately constant with pressure and temperature, i.e., SuB, $Mg_{10}Si_3O_{18}H_4$; phase G, $Mg_{1.14}Si_{1.73}H_{2.82}O_6$, although the Mg/Si ratios, together with water contents in superhydrous phase B and hydrous phase G, vary with pressure and temperature. The small amount of water contents in ilmenite,

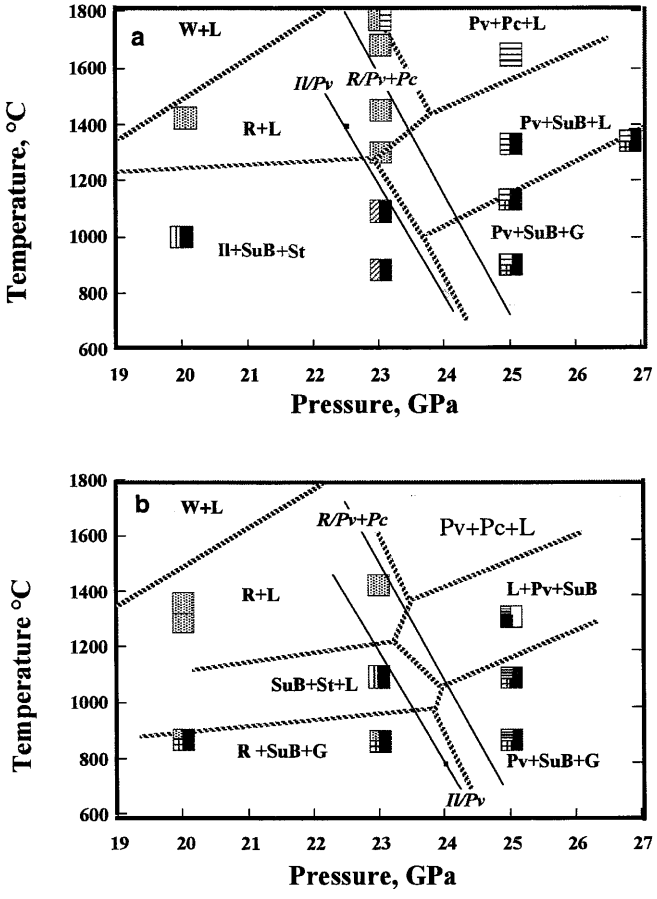

Fig. 6a, b Phase relation for the Mg_2SiO_4-5 wt% H_2O bulk composition (**a**) and that for the Mg_2SiO_4-11 wt% H_2O bulk composition (**b**) *R* ringwoodite; *Pc* periclase; other abbreviations are the same as those used in Fig. 5

Table 2 Experimental conditions and results in the Mg_2SiO_4-H_2O system. *R* Hydrous ringwoodite; *Il* ilmenite; *Pv* perovskite; *Pc* periclase; *St* stishovite; *L* liquid; *G* phase G; *SuB* superhydrous phase B

Run no.	Pressure (GPa)	Temperature (°C)	Time (h)	Results
Mg_2SiO_4-5 wt% H_2O bulk composition				
F5H22	20	1000	30	SuB + St(+Il)[a]
F5H21	20	1450	3	R + L
F5R16	23	880	30	Il + SuB(+St)[a]
F5H27	23	1100	30	Il + SuB(+St)[a]
F5H11	23	1300	3	R + L
F5H09	23	1450	3	R + L
F5H15	23	1680	3	R + L
F5H26	23	1800	1	R + Pv + L
F5H14	25	900	30	Pv + SuB + G
F5H08	25	1130	3	Pv + SuB(+trace G)
F5H06	25	1330	3	Pv + SuB + L
F5H12	25	1650	3	Pv + Pc + L
F5H17	25	1980	1	Pv + Pc + L
F5H28	27	1300	3	Pv + SuB(+trace G)
Mg_2SiO_4-11 wt% H_2O bulk composition				
F11H09	20	880	24	R + SuB + trace G
F11H04	20	1300	1	R + L
F11H05	20	1370	1	R + L
F11H10	23	880	27	R + SuB + G
F11H03	23	1100	3	SuB + St + L
F11H06	23	1450	1	R + L
F11H02	25	880	10	Pv + SuB + G
F11H08	25	1100	3	Pv + SuB + L SuB + trace G + L
F11H01	25	1320	3	Pv + SuB + L

[a] The phase is not observed, but expected to exist based on mass balance

stishovite, and perovskite was also ignored in this approximation.

Mg_2SiO_4-11 wt% H_2O system

We carried out experiments in the Mg_2SiO_4-11 wt% H_2O system in the pressure range from 20 to 25 GPa and the temperature range from 850 to 1400 °C. Phase G coexists with superhydrous phase B in the pressure range of 20 ~ 25 GPa at 900 °C, and the stability field of phase G in this system expands into the lower pressure range compared to that of the Mg_2SiO_4-5 wt% H_2O system.

Superhydrous phase B appears above 20 GPa, which is similar to the Mg_2SiO_4-5 wt% H_2O bulk composition. Superhydrous B, stishovite, and fluid coexist at 23 GPa and 1100 °C, whereas superhydrous phase B coexists with $MgSiO_3$, perovskite, and liquid at 25 GPa and 1100 °C. At higher temperatures around 1300–1400 °C, hydrous ringwoodite (γ-Mg_2SiO_4) and liquid are stable at 20 GPa, whereas superhydrous phase B, $MgSiO_3$ perovskite, and liquid coexist at 25 GPa. The chemical composition of the liquid coexisting with superhydrous phase B and $MgSiO_3$ perovskite at 25 GPa and 1320 °C (Run F11H01), determined by EPMA analysis, is about 48 wt% MgO, 10 wt% SiO_2, and about 42 wt% H_2O estimated by the wt% deficiency in the EPMA analyses of the quench liquid. The highly magnesian nature of the quench liquid determined here is consistent with the results by Frost and Fei (1998). Thus, the partition coefficient of water between superhydrous phase B and liquid is estimated to be 0.15 at 25 GPa and 1320 °C. Superhydrous phase B and phase G are stable in the cold slabs descending into the upper part of the lower mantle under locally water-enriched conditions.

The reaction between R + SuB + G and Pv + SuB + G occurs at around 25 GPa. This reaction can be reduced to the following reaction, R + 0.18G = 0.93Pv + 0.13SuB by assuming constant chemical compositions of ringwoodite, phase G, superhydrous phase B, and perovskite at various pressures and temperatures.

Water content in hydrous ringwoodite (γ-Mg_2SiO_4)

Water content in hydrous ringwoodite was measured by secondary ion mass spectrometry (SIMS). We used San Carlos olivine and natural hornblende as the standard materials for the SIMS analysis. The H_2O contents in hydrous ringwoodite are summarized in Table 3. The matrix effects are ignored since the SiO_2 contents in the standard materials are close to ringwoodite. The errors given in Table 3 are caused by the errors in the estimation of the H_2O content in the standard material of natural hornblende, 0.1 wt%, and the reproducibility and variation of background for the SIMS analysis, which are within about 10% of the measured values.

The estimated partition coefficients of water between hydrous ringwoodite and liquid are also given in Table 3. In the runs conducted at 23 GPa and 1450 °C (F11H06), we observed a large pool of quenched silicate liquid, whose composition was determined by EPMA to be MgO 53.88 wt%, SiO_2 7.54%, and H_2O 38.58%, where the water content was estimated by the wt% deficit of the analysis total. The water contents of the liquid in the other runs were estimated based on the volume fraction of hydrous ringwoodite and liquid and the composition of hydrous ringwoodite. This result implies that the partition coefficient of water between hydrous ringwoodite and liquid, D(R/L), is about 0.02 ~ 0.04 at 20 ~ 23 GPa and about 1300 ~ 1450 °C, and it decreases with increasing temperature.

Inoue et al. (1997) synthesized hydrous ringwoodite (γ-Mg_2SiO_4) coexisting with liquid and stishovite in the composition of Mg_2SiO_4-11 wt% H_2O at 19 GPa and 1300 °C. They determined the water content of the hydrous ringwoodite to be 2.2 wt%. In the Mg_2SiO_4-11 wt% H_2O bulk composition at 20 ~ 23 GPa and 1300 ~ 1450 °C, hydrous ringwoodite (γ-Mg_2SiO_4) contains about 1.5 ~ 2.6 wt% H_2O, which is consistent

Table 3 The H_2O content in hydrous ringwoodite and the coexisting liquid. *R + Liq* hydrous ringwoodite + liquid

Run no.	Pressure (GPa)	Temperature (°C)	Phases present	Mg/Si (atm) in hydrous ringwoodite	H_2O content (wt%)[a] in hydrous ringwoodite	H_2O content (wt%) in liquid	Partition coefficient, D (R/L)
F11H04	20	1300	R + Liq	1.96(0.05)	2.6(0.2)	100[b]	0.025
				1.94(0.05)	2.4(0.2)		0.024
F11H05	20	1370	R + Liq	1.95(0.02)	1.9(0.13)	68.5 ~ 83.4[c]	0.021 ~ 0.026
				1.95(0.04)	1.7(0.12)		0.02 ~ 0.025
F11H06	23	1450	R + Liq	1.96(0.05)	1.6(0.13)	38.6[d]	0.04
				1.97(0.03)	1.7(0.13)		0.044
				1.97(0.03)	1.5(0.11)		0.039
F5H15	23	1680	R + Liq	1.96(0.07)	0.2(0.04)	[e]	–
F5H26	23	1800	R + Liq	1.97(0.01)	0.3(0.02)	[e]	–

[a] Determined by SIMS
[b] Assumed
[c] Calculated by the mass balance and the ringwoodite composition
[d] Estimated by the EPMA analysis total
[e] Not determined

Table 4 Compositions of the coexisting phases in some runs

Run no.	Press. (GPa)	Temp. (°C)	Phases	MgO (wt%)	Error[a]	SiO_2 (wt%)	Error[a]	Total	Mg/Si (atom)
Mg_2SiO_4-5 wt% H_2O									
F5H22	20	1000	SuB	64.59	0.18	29.21	0.09	93.8	3.29
F5R16	23	880	Il	39.02	0.66	60	0.39	99.03	0.97
			SuB	64.66	0.31	29.61	0.31	94.27	3.26
F5H27	23	1100	Il	39.68	0.77	60.46	0.04	100.14	0.98
			SuB	65.32	0.45	29.32	0.24	94.64	3.325
F5H14	25	900	Pv	41.78	0.23	62.27	0.27	104.05	1.0001
			SuB	64.05	0.72	29.39	0.6	93.44	3.25
			G	28.75	0.66	63.39	0.1	95.25	0.675
Mg_2SiO_4-11 wt% H_2O									
F11H09	20	880	R	55.55	0.05	42.25	0.03	97.8	1.96
			SuB	64.26	0.05	29.21	0.3	93.47	3.18
			G	28.14	0.27	61.05	0.37	89.18	0.69
			D_{H_2O} (R/SuB) = 0.336[b]						
			D_{H_2O} (R/G) = 0.203						
F11H10	23	880	R	56.8	0.27	42.03	0.18	98.83	2.01
			SuB	64.69	0.49	29.55	0.26	94.24	3.26
			G	29.92	0.32	60.92	0.42	90.84	0.73
			D_{H_2O} (R/SuB) = 0.203						
			D_{H_2O} (R/G) = 0.128						
F11H03	23	1100	SuB	65.14	0.4	28.88	0.27	94.02	3.36
F11H02	25	880	Pv	42.24	0.3	61.57	0.38	103.81	1.02
			SuB	63.73	0.41	29.06	0.27	92.81	3.27
			G	29.14	1.43	60.07	2.68	89.22	0.73
E15H01	25	1150	SuB	64.1	0.29	29.32	0.2	93.42	3.26
			G	28.17	1.34	58.78	0.69	86.95	0.72
			D_{H_2O} (SuB/G) = 0.504						
E15H03	23	1300	SuB	66.16	0.41	29.43	0.27	95.59	3.35
			G	28.94	1.11	60.92	1.96	89.87	0.71
			D_{H_2O} (SuB/G) = 0.435						
E15H09	20	880	SuB	65.41	0.42	29.23	0.28	94.54	3.35
			G	29.01	0.29	58.43	0.37	87.45	0.74
			D_{H_2O} (SuB/G) = 0.435						
E15H04	20	1100	SuB	64.61	0.42	29.18	0.28	93.79	3.3
			G	25.66	0.08	65.94	0.19	91.59	0.58
			D_{H_2O} (SuB/G) = 0.738						
E15H08	23	1300	SuB	64.38	0.42	27.86	0.27	92.24	3.44
			G	26.28	0.27	64.51	0.39	90.79	0.61
			D_{H_2O} (SuB/G) = 0.843						

[a] 1σ error
[b] The partition coefficients of water were based on the water content estimated from the analysis total

with the result of Inoue et al. (1997). The changes in water content in hydrous ringwoodite with temperature at 20 $\sim$ 23 GPa are shown in Fig. 7. Water contents in hydrous ringwoodite are less than 0.3 wt% at 23 GPa and above 1600 °C. The present observation implies that water content in hydrous ringwoodite decreases with increasing temperature.

Kawamoto et al. (1996) determined the water content in hydrous ringwoodite to be about 0.7 wt% at 15.5 GPa and 1300 °C in the KLB1-3.4 wt% H_2O system by SIMS measurement. This is consistent with the present results. These results suggest that the amount of water retained in hydrous ringwoodite in the mantle might be equivalent to that retained in hydrous wadsleyite (β-Mg_2SiO_4).

The relationship between Mg/Si ratio and water content for hydrous ringwoodite is shown in Fig. 8. The relation for wadsleyite (Inoue et al. 1995) is also shown in the same figure. We observe a clear difference in dependency of water content with the Mg/Si ratio between hydrous ringwoodite and hydrous wadsleyite. This observation suggests that hydrogen ions H^+ in hydrous ringwoodite locate in different sites from those of hydrous wadsleyite.

The IR spectrum of hydrous ringwoodite is shown in Fig. 9, and is consistent with that reported by Kohldstedt et al. (1996) and Kagi et al. (1997). The broad absorption peaks observed at around 3100 cm^{-1} are in the range of the OH-stretching vibration and those observed at 1600 cm^{-1} are assumed to be caused by the HOH-bending vibration mode by Kagi et al. (1997), who argued that molecular water in hydrous ringwoodite (γ-Mg_2SiO_4) could occur both as fluid inclusions and/or as structurally bound molecular water based on the IR spectrum.

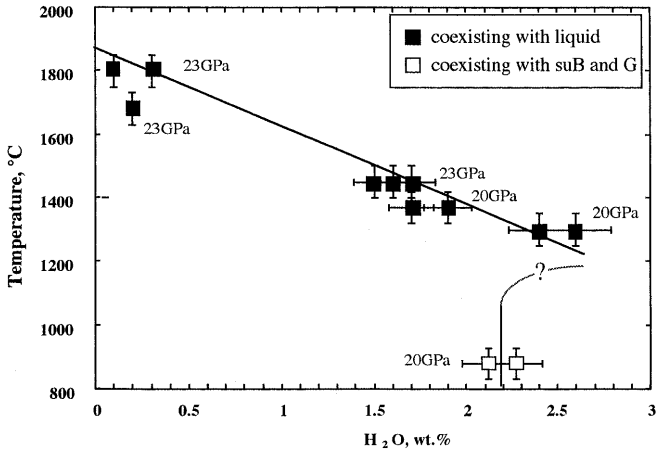

Fig. 7 The change in the H_2O content of hydrous ringwoodite with temperature at 20 ~ 23 GPa

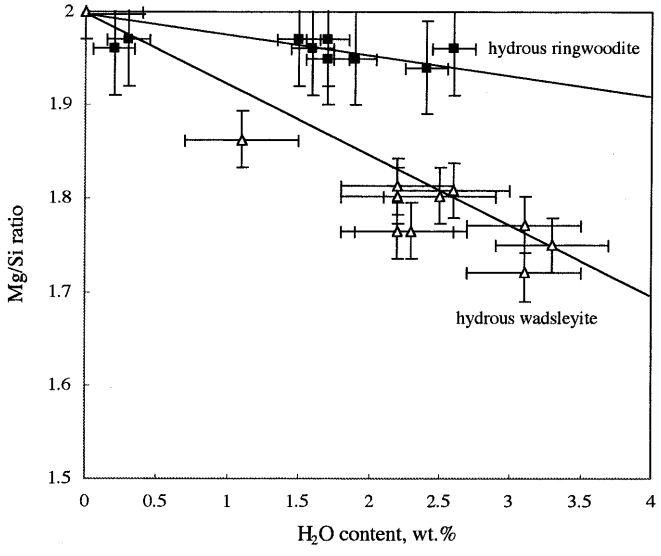

Fig. 8 Relation between Mg/Si ratio and water in hydrous ringwoodite (present work) and hydrous wadsleyite (Inoue et al. 1995)

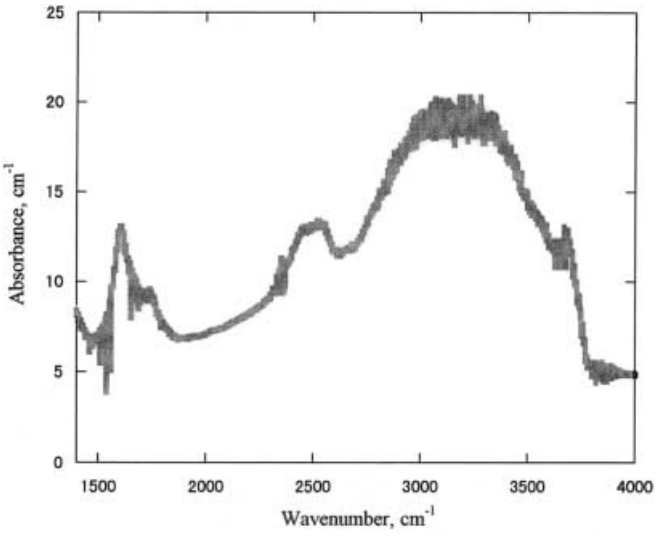

Fig. 9 IR spectrum of hydrous ringwoodite synthesized at 20 GPa and 1300 °C (Run F11H04), containing 2.6 wt% of H_2O

Discussion

Identification of dense hydrous magnesium silicates (DHMS)

Ringwood and Major (1967) investigated the system Mg_2SiO_4-MgO-H_2O at pressures of 10–18 GPa and reported phases A, B, and C. The stability field of phase A was determined by several authors (e.g., Luth 1995). Crystal structures of phases A and B were reported by Horiuchi et al. (1979) and Finger et al. (1991), respectively.

In spite of the effort to simplify the nomenclature of the DHMS phases, some ambiguities still remain. Superhydrous phase B was discovered by Gasparik (1990) at 15–23 GPa, and named on the basis of the chemical composition of the phase. Later, Pacalo and Parise (1992) clarified the crystal structure of the phase and found that it belongs to the space group Pnnm. Kanzaki (1993) suggested that superhydrous phase B may be identical to phase C (Ringwood and Major 1967) on the basis of the X-ray diffraction data. On the other hand, Kudoh et al. (1994) reported that the crystal structure of superhydrous phase B synthesized by Kanzaki (1991) belongs to the space group P21nm, which is different from that reported by Pacalo and Parise (1992). Therefore, there may be two different phases of superhydrous phase B, as was suggested by Burnley and Navrotsky (1996). Further work is needed for the characterization of superhydrous phase B.

Ohtani et al. (1997) reported that phase G exists in the $MgSiO_3$-H_2O system at 22 GPa and 1050 °C, and it contains 14.5 ± 2.0 wt% H_2O based on the SIMS measurement. The Mg/Si atomic ratio of the phase was determined to be 0.65 ~ 0.75 by EPMA analysis. The chemical formula of phase G is $Mg_{1.14}Si_{1.73}H_{2.81}O_6$. Ohtani et al. (1995, 1998) reported the stability of the assemblages phase G + brucite and phase G + superhydrous phase B in the Mg_2SiO_4-20.4 wt% bulk composition at around 20 ~ 25 GPa and 900 ~ 1100 °C.

Kudoh et al. (1997) reported the structure of a single crystal of phase G that was synthesized at 22 GPa and 1050 °C. The results of the structural analysis indicated that phase G had a trigonal symmetry with the unit cell, a = 4.790(3) Å, c = 4.344(3) Å, V = 86.3(2) Å^3. According to their work, phase G is composed of two layers, the S-layer of $(Si_{0.88}Mg_{0.12})O_6$ octahedra and the M-layer of MgO_6 octahedra in direction along the c-axis. The most significant characteristic of the structure of phase G is that it is composed of six-coordinated Si ions with few four-coordinated Si ions. The structure of phase G is close to that of stishovite SiO_2. The calculated X-ray density of phase G is 3.43 g cm^{-3}, which is denser

than any other DHMS phases, although it contains a large amount of water.

Yang et al. (1997) independently reported the crystal structure of the same hydrous phase, $Mg_{1.11}Si_{1.89}H_{2.22}O_6$, synthesized in the system Mg_2SiO_4-H_2O at 20 GPa and 1200 °C, and they called it phase D on the basis of the similarity of the X-ray diffraction pattern with the original phase D by Liu (1987). The synthesis conditions and phase relations in the system are given in Frost and Fei (1998), who redefined phase D assuming that the original X-ray data of phase D observed by Liu (1987) and Li and Jeanloz (1991) contained some contaminant phases although they could not specify these. Kuroda and Irifune (1998) also reported a similar phase in the products of the decomposition of serpentine. Phase D, redefined by Yang et al. (1997), will be identical to phase G in this manuscript. Although they preferred to use the term phase D, we adopt here the name phase G instead of phase D, in order to avoid the confusion associated with the name phase D. There is some confusion in the name of phase D, i.e., we cannot yet deny the possibility of the existence of the original phase D defined by Liu (1987). Further, the name phase D, as introduced by Yamamoto and Akimoto (1974, 1977), is a pure form of hydroxy-chondrodite without Ti and F, and some authors used the name phase D for this (e.g., Finger et al. 1991; Prewitt and Finger 1992; Schreyer 1995). It is likely that the phase F reported by Kanzaki (1991) is identical with the present phase G, as was discussed by some authors (e.g., Frost and Fei 1998; Ohtani et al. 1998).

Stability of phase G and superhydrous phase B

The stability relations of the MgO-SiO_2-H_2O system are summarized in Fig. 10 in the pressure range from 15 to 27 GPa. In this figure, we summarize the phase relations

Fig. 10 The stability relations of the MgO-SiO_2-H_2O system in the pressure ranges from 15 to 25 GPa. This figure summarizes experimental results determined in this work, Ohtani et al. (1997), Ohtani et al. (1995), Frost and Fei (1998), those in the MgO-SiO_2-H_2O system reported by Gasparik (1993) and Kanzaki (1991), and those in the serpentine bulk composition by Kuroda and Irifune (1998)

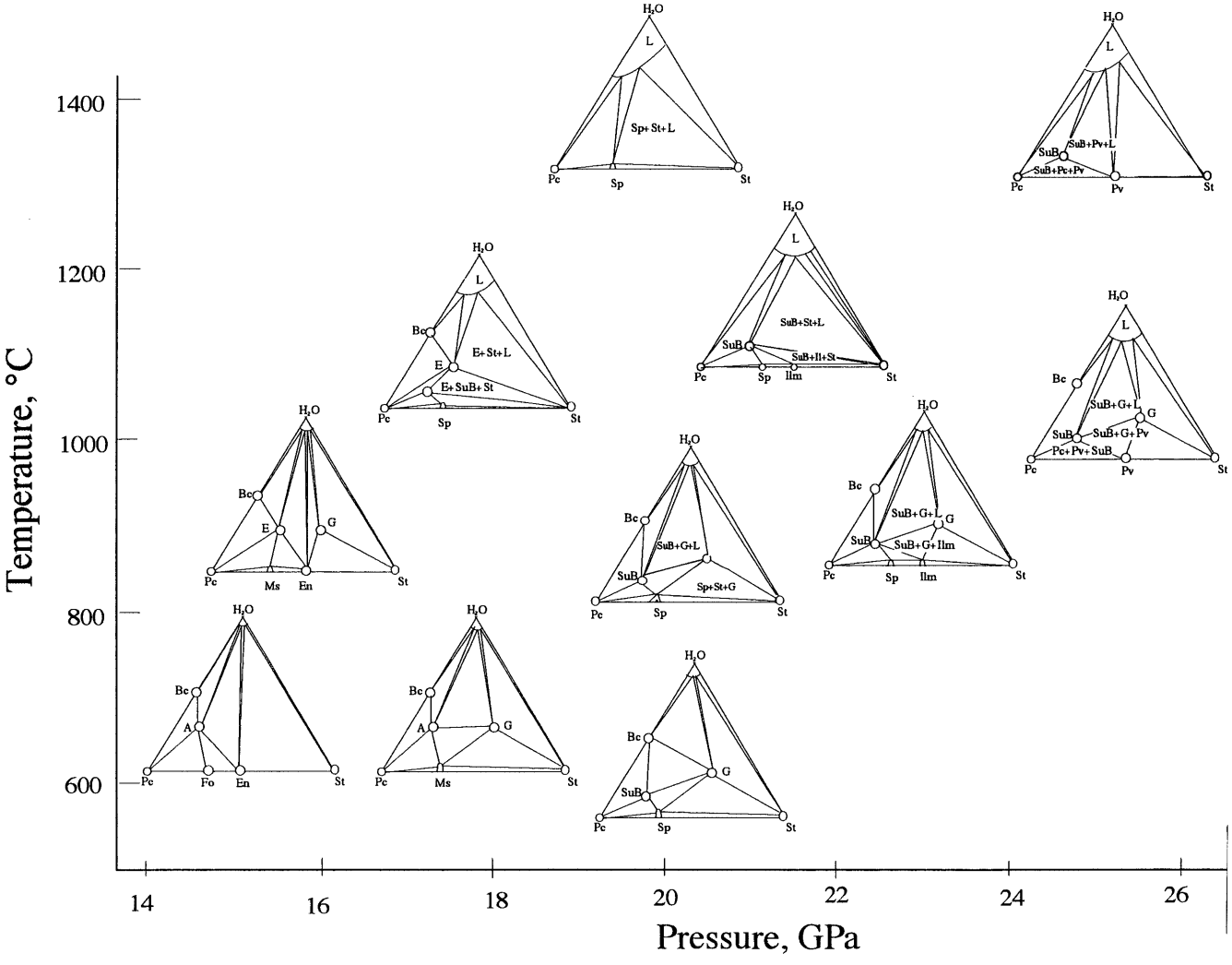

of the $MgSiO_3$-H_2O system determined in this work and in Ohtani et al. (1997), those of the Mg_2SiO_4-H_2O system in this work, Ohtani et al. (1995), and Frost and Fei (1998), those in the MgO-SiO_2-H_2O system by Kanzaki (1991) and Gasparik (1993), and those in the serpentine bulk composition by Kuroda and Irifune (1998). This figure suggests that the stability field of phase G expands in the system with high water content and low Mg/Si ratios.

Recent studies using the diamond anvil cell indicate that superhydrous phase B is stable up to 30 GPa, whereas phase G decomposes to periclase, $MgSiO_3$ perovskite, and fluid at around 40 GPa (Shieh et al. 1998). Thus, superhydrous phase B and phase G may be the major host phases of water in the cold slabs subducting into the uppermost part of the lower mantle and deep into the lower mantle, respectively.

Partitioning of water among hydrous phases and liquid

We observed the coexistence of hydrous ringwoodite, superhydrous phase B, and phase G in the Mg_2SiO_4-11 wt% H_2O bulk composition. The partition coefficient of water between hydrous ringwoodite and superhydrous phase B, D(R/SuB), is around 0.13 $\sim$ 0.34 at 20 $\sim$ 23 GPa and 880 °C, and it decreases slightly with increasing pressure. On the other hand, the partition coefficient of water between hydrous ringwoodite and phase G, D(R/G), is about 0.2 at 20 GPa and 880 °C, and it decreases with increasing pressure. The pressure dependencies of the partition coefficients at 880 °C are given in Fig. 11a. These results imply that water preferentially partitioned into phase G and superhydrous phase B relative to hydrous ringwoodite, and the partition coefficients, D(R/SuB) and D(R/G), decreases with increasing pressure.

Coexistence of phase G, superhydrous phase B, and fluid was observed in the $MgSiO_3$-15 wt% H_2O system in the pressure and temperature ranges of 20 $\sim$ 25 GPa and 880 $\sim$ 1300 °C, as is shown in Fig. 6b. The partition coefficients between superhydrous phase B and phase G, D(SuB/G), is about 0.73 at 20 GPa and 1100 °C, and it decreases with increasing pressure and increases with increasing temperature, as shown in Fig. 11b. This observation implies that water preferentially favors phase G relative to superhydrous phase B with increasing pressure and decreasing temperature.

The partition coefficient of water between hydrous ringwoodite and liquid, D(R/L), is about 0.02 $\sim$ 0.04 at 20 $\sim$ 23 GPa and about 1300 $\sim$ 1450 °C, and it decreases with increasing temperature. The partition coefficient values are consistent with that estimated by Kawamoto et al. (1996), 0.04 at 15.5 GPa and 1300 °C. The partition coefficient of water between superhydorus phase B and liquid, D(SuB/L), was estimated to be 0.15 at 25 GPa and 1320 °C, as was described previously.

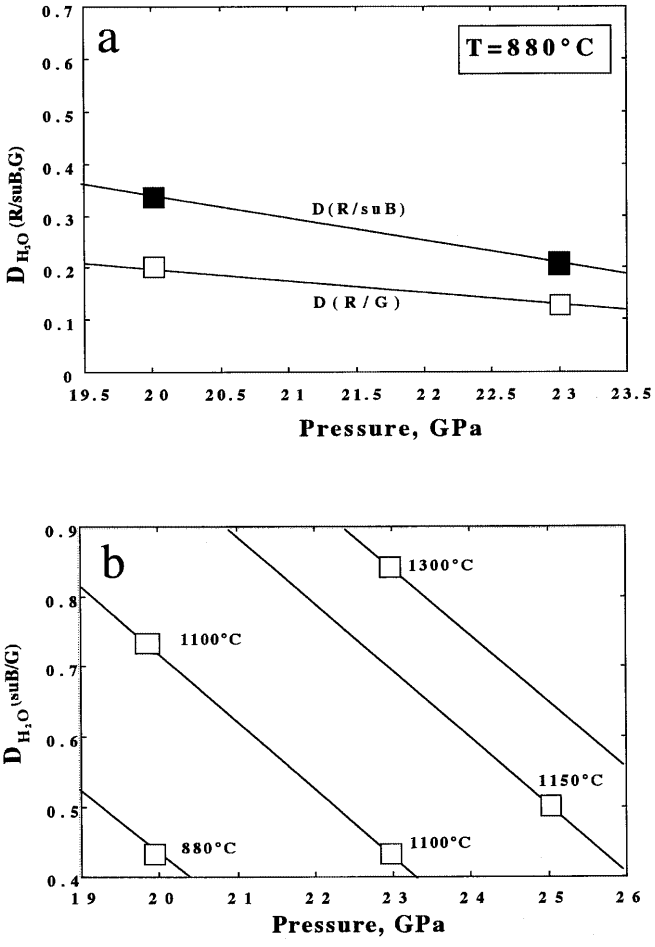

Fig. 11a, b The change with pressure and temperature of the partition coefficients of water between hydrous minerals. **a** Partition coefficients between hydrous ringwoodite and hydrous phase G, $D(R/G)$, and hydrous ringwoodite and superhydrous phase B, $D(R/SuB)$. **b** Partition coefficients between superhydrous phase B and hydrous phase G, $D(SuB/G)$ coexisitng with the liquid

Stability of dense hydrous magnesium silicates and H_2O storage capacity in the mantle

The stability of dense hydrous magnesium silicates (DHMS) in the MgO-SiO_2-H_2O system under mantle conditions has been investigated by many workers. DHMS phases are not stable at temperatures corresponding to the mantle geotherm, but are stable under subduction zone conditions (Gasparik 1993). According to the previous works, temperatures in the coldest part of the old slabs may be as low as about 400 $\sim$ 700 °C at the 200-km depth, 600 $\sim$ 800 °C at the 410-km seismic discontinuity, and about 600 $\sim$ 700 °C at the 670-km discontinuity (e.g., Helffrich and Brodholt 1991).

The stability of the hydrous phases expected to exist in the descending slabs are schematically shown in Fig. 12. The hydrous phases present in the sediment and basalt layers in the slabs are not shown in this figure. Along the geotherm of the cold slabs, serpentine (antigorite) breaks down, and phase A appears by the reaction; antigorite = phase A + clinoenstatite + fluid

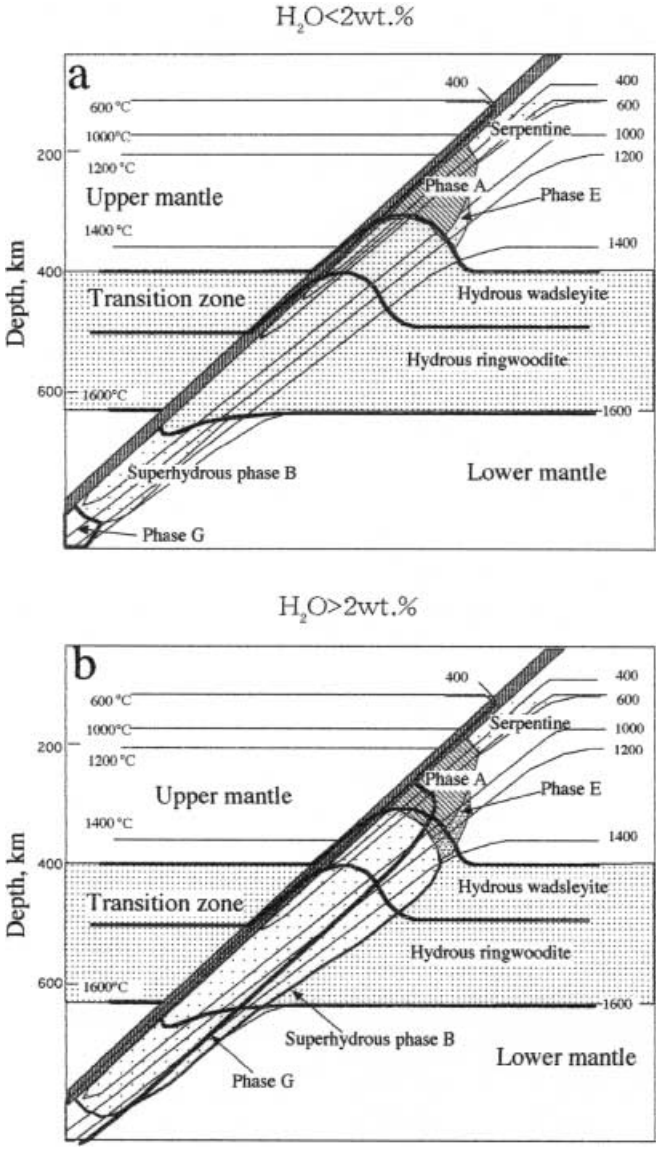

Fig. 12a, b The stability of hydrous phases in the peridotite layer of the descending slabs with H_2O less than about 2 wt% (**a**) and with H_2O more than 2 wt% (**b**). The hydrous phases in the sediment and basalt layers are not shown

at 7 GPa and 600 °C (Ulmer and Trommsdorff 1995). Stability of phase A was also reported by Luth (1995). Host minerals of H_2O in subducting slabs may change with temperature and the H_2O contents in the slabs. In the slabs with H_2O content less than about 2 wt%, phase A carries water up to a depth of 450 km. Hydrous wadsleyite, hydrous ringwoodite, and ilmenite are the main H_2O reservoirs in the transition zone of the depths from 450 to 660 km. The stability field of ringwoodite may expand into higher pressures under wet conditions, as was discussed in the previous section, although more careful determination of the stability field of hydrous ringwoodite is needed. Superhydrous phase B is the H_2O reservoir in the cold slabs subducting into the uppermost part of the lower mantle of depths from 670 to 800 km, whereas phase G appears in the slabs in the lower mantle only at depths greater than 800 km.

In the cold slabs with local water saturation, on the other hand, the following hydrous phases appear with increasing depth; phase A to 450 km depth, phase A and phase G from 450 to 550 km, brucite, superhydrous phase B, and phase G from 550 to 800 km, and phase G at depths greater than 800 km.

In the upper mantle, olivine can accommodate only a limited amount of about 1090 ppm of H_2O at about 13 GPa and 1100 °C, although the amount of water stored in olivine increases with pressure (Kohlstedt et al. 1996). The small amount of H_2O, however, has a great effect on its rheology, i.e., hydrolytic weakening (e.g., Karato 1986).

The major constituent minerals in the transition zone, wadsleyite and ringwoodite, can accommodate a large amount of about 2 wt% of H_2O at 1000 $\sim$ 1200 °C, and at least up to about 0.1 wt% of H_2O at 1600 °C. The maximum H_2O storage potential of wadsleyite and ringwoodite is estimated to be about 0.1 $\sim$ 1 wt% along the normal geotherm (e.g., Inoue and Sawamoto 1992; Kawamoto and Holloway 1997).

The lower mantle minerals such as Mg-perovskite do not contain significant H_2O; preliminary results imply that the H_2O content in Mg-perovskite synthesized at 1600 °C under the hydrothermal conditions is only about 100 ppm (Meade et al. 1994). Both superhydrous phase B and phase G in the lower mantle decompose at a temperature around 1500 °C (Shieh et al. 1998). Thus, the water storage potential will be very small at the lower mantle conditions.

There is a possible layered structure of the mantle in terms of its water-storage capacity; i.e., the upper and lower mantles have relatively small water-storage capacities, whereas the transition zone has a larger capacity. Thus, the water content in the transition zone might be large because the primordial water trapped in the lower mantle and the recycled water circulated due to the slab subduction have been stored in the transition zone during geological time.

Summary

High-pressure and -temperature phase equilibria in the system of MgO-SiO_2-H_2O were investigated in the pressure range from 20 to 27 GPa.

1. Phase equilibrium studies in the systems $MgSiO_3$-15 wt% H_2O, Mg_2SiO_4-5 wt% H_2O, and Mg_2SiO_4-11 wt% H_2O revealed that phase E, phase G, and superhydrous phase B appear as DHMS phases in the pressure range from 20 to 25 GPa in these systems. The stability field of phase G expands with increasing H_2O contents and decreasing the Mg/Si ratio of the system.

2. The H_2O contents in hydrous ringwoodite (γ-Mg_2SiO_4) coexisting with the liquid decrease with increasing temperature; from 1.5 $\sim$ 2.6 wt% H_2O at 1300 $\sim$ 1400 °C and 20 $\sim$ 23 GPa to about 0.3 wt% at

1700 ~ 1800 °C and 23 GPa. Partition coefficient of H_2O between ringwoodite and superhydrous phase B, D(R/SuB), is about 0.34 at 20 GPa and 880 °C, and decreases with increasing pressure. Partition coefficient of H_2O between ringwoodite and phase G, D(R/G), is about 0.2 at 20 GPa and 880 °C, and decreases with increasing pressure. Partition coefficient of H_2O between superhydrous phase B and phase G, D(SuB/G), is about 0.73 at 20 GPa and 1100 °C, and it decreases with increasing pressure and with decreasing temperature. The partition coefficient of H_2O between hydrous ringwoodite and liquid, D(R/L), is around 0.04, which is smaller than that between wadsleyite and liquid, D(Wad/L), estimated by Kawamoto et al. (1996) to be 0.1.

3. Water stored in serpentine in the cold descending slabs can be transported into depths greater than 200 km. Serpentine decomposes to a mixture of phase A, enstatite, and fluid. In the slabs with H_2O content less than about 2 wt%, the following hydrous phases appear with depth: phase A carries water up to a depth of 450 km. Hydrous wadsleyite, hydrous ringwoodite, and ilmenite are the main H_2O reservoirs in the transition zone from 450 to 660 km depth. The stability field of hydrous ringwoodite may expand into higher pressures relative to anhydrous ringwoodite. Superhydrous phase B is the H_2O reservoir in the uppermost part of the lower mantle from 660 to 800 km, whereas phase G appears in the lower mantle only at depths greater than 800 km. In the cold slabs with local H_2O saturation, the following hydrous phases appear with increasing depths: phase A to 450 km, phase A and phase G from 450 to 550 km, brucite, superhydrous phase B, and phase G from 550 to 800 km, and phase G at the depths greater than 800 km.

Acknowledgements We appreciate the help of T. Kondo and T. Yagi in making X-ray diffraction measurements of the run products using the micro-area X-ray diffractometer. We thank A. Suzuki for helpful assistance and useful discussions during the experiments. We thank Y. Ito for EPMA analysis. We also thank T. Terada and M. Akizuki for providing a chance to use the micro-IR spectrometer, and S. Yamagata of JASCO Co. Ltd. for measuring the run products by the micro-Raman spectrometer. We also appreciate T. Gasparik for his critical review for improving this manuscript. This work was partially supported by the grant-in-aid for Scientific Research (A) of the Ministry of Education, Science, Sport, and Culture of the Japanese government, no. 09304051 to E. Ohtani.

References

Burnley PC, Navrotsky A (1966) Synthesis of high-pressure hydrous magnesium silicates: observations and analysis. Am Mineral 81: 317–326

Finger LW, Hazen RM, Prewitt CT (1991) Crystal structures of $Mg_{12}Si_4O_{19}(OH)_2$ (phase B) and $Mg_{14}Si_5O_{24}$ (phase AnhB). Am Mineral 76: 1–7

Frost DJ, Fei Y (1998) The stability of phase D at high pressure and temperature. J Geophys Res 103: 7463–7474

Gasparik T (1990) Phase relations in the transition zone. J Geophys Res 95: 15751–15769

Gasparik T (1993) The role of volatiles in the transition zone. J Geophys Res 98: 4287–4299

Helffrich G, Brodoholt J (1991) Relationship of deep seismicity to the thermal structure of subducted lithosphere. Nature 353: 252–255

Horiuchi H, Morimoto N, Yamamoto K, Akimoto S (1979) Crystal structure of $2Mg_2SiO_43Mg(OH)_2$, a new high-pressure structure type. Am Mineral 64: 593–598

Inoue T, Sawamoto H (1992) High-pressure melting of pyrolite under hydrous conditions and its geophysical implications. In: Syono Y, Manghnani MH (eds) High pressure research: application to earth and planetary sciences. Terra, Tokyo and AGU, Washington, DC, pp 323–331

Inoue T, Yurimoto H, Kudoh Y (1995) Hydrous modified spinel, $Mg_{1.75}SiH_{0.5}O_4$: a new water reservoir in the mantle transition region. Geophys Res Lett 22: 117–120

Inoue T, Chen J, Weidner DJ, Kagi H, Yurimoto H, Northrup PA, Parise JB (1997) Phase boundaries between olivine (α) hydrous wasleyite (β) and hydrous ringwoodite (γ), and their elastic properties (abstract). In: Special issue of Rev High-Press Sci Technol 6, 489 p

Ito E, Takahashi E (1989) Postspinel transformations in the system Mg_2SiO_4-Fe_2SiO_4 and some geophysical implications. J Geophys Res 94: 10637–10646

Kagi H, Inoue T, Weidner DJ, Lu R, Rossman GR (1997) Speciation of hydroxides in hydrous phases synthesized at high pressure and temperature (abstract). In: 1997 Jpn Earth Planet Sci Joint Meeting Abstr, pp 506 (in Japanese)

Kanzaki M (1991) Stability of hydrous magnesium silicates in the mantle transition zone. Phys Earth Planet Inter 66: 307–312

Kanzaki M (1993) Calculated powder X-ray patterns of phase B, anhydrous B and superhydrous B: re-assessment of previous studies. Mineral J 16: 278–285

Karato S (1986) Does partial melting reduces the creep strength of the upper mantle? Nature 319: 309–310

Kato T, Ohtani E, Morishima H, Yamazaki D, Suzuki A, Suto M, Kubo T, Kikegawa T, Shimomura O (1995) In situ X-ray observation of high-pressure phase transitions of $MgSiO_3$ and thermal expansion of $MgSiO_3$ perovskite at 25 GPa by double-stage multianvil system. J Geophys Res 100: 20475–20481

Kawai N, Endo S (1970) The generation of ultrahigh hydrostatic pressures by a split sphere apparatus. Rev Sci Instrum 41: 1178–1181

Kawamoto T, Herig RL, Holloway JR (1996) Experimental evidence for a hydrous transition zone in the early Earth's mantle. Earth Planet Sci Lett 142: 587–592

Kawamoto T, Holloway JR (1997) Melting temperature and partial melt chemistry of H_2O-saturated mantle peridotite to 11 gigapascals. Science 276: 240–243

Kohlstedt DL, Keppler H, Rubie DC (1996) Solubility of water in the α, β and γ phases of $(Mg,Fe)_2SiO_4$. Contrib Mineral Petrol 123: 345–357

Kubo T, Ohtani E, Kato T, Shinmei T, Fujino K (1998) Effects of water on the α-β transformation kinetics in San Carlos olivine. Science 281: 85–87

Kudoh Y, Nagase T, Ohta T, Sasaki S, Kanzaki M, Tanaka M (1994) Crystal structure and compressibility of superhydrous phase B, $Mg_{20}Si_6H_8O_{36}$. In: Schmidt SC, Shaner JW, Samara GA, Ross M (eds) High-pressure science and technology, 1993. Am Inst Phys. New York

Kudoh Y, Nagase T, Mizobata H, Ohtani E, Sasaki S, Tanaka M (1997) Structure and crystal chemistry of phase G, a new hydrous magnesium silicate synthesized at 22 GPa and 1050 °C. Geophys Res Lett 24: 1051–1054

Kuroda K, Irifune T (1998) Observation of phase transformations in serpentine at high pressure and high temperature by in situ X ray diffraction measurements. In: Manghnani MH, Yagi T (eds) High-pressure-temperature research: properties of earth and planetary materials. Geophysical Monograph 101, Am Geophys Union, Washington, DC, pp 545–554

Kurosawa M, Yurimoto H, Matsumoto K, Sueno S (1992) Hydrogen analysis of mantle olivine by secondary ion mass spectrometry. In: Syono Y, Manghnani MH (eds) High-pres-

sure research: application to earth and planetary sciences. Am Geophys Union, Washington, DC, pp 283–287
Li X, Jeanloz R (1991) Phases and electrical conductivity of a hydrous silicate assemblage at lower mantle conditions. Nature 350: 332–334
Liu LG (1987) Effect of H_2O on the phase behavior of the forsterite-enstatite system at high pressures and temperatures and implications for the Earth. Phys Earth Planet Inter 49: 142–167
Luth RW (1995) Is phase A relevant to the Earth's mantle? Geochim Cosmochim Acta 59: 679–682
Meade C, Reffner JA, Ito E (1994) Synchrotron infrared absorbance measurements of hydrogen in $MgSiO_3$ perovskite. Science 264: 1558–1560
Miyagi I, Yurimoto H (1995) Water content of melt inclusions in phenocrysts using secondary ion mass spectrometer. Bull Volcanol Soc Jpn 40: 349–355
Ohtani E, Suzuki A, Kato T (1998) Flotation of olivine and diamond in mantle melt at high pressure: implications for fractionation in deep mantle and ultradeep origin of diamond. In: Manghnani MH, Yagi T (eds) High-pressure research: properties of earth and planetary materials at high pressure and temperature. Geophysical Monograph 101, Am Geophys Union, Washigton, DC, pp 227–239
Ohtani E, Shibata T, Kubo T, Kato T (1995) Stability of hydrous phases in the transition zone and the upper most part of the lower mantle. Geophys Res Lett 22: 2553–2556
Ohtani E, Mizobata H, Kudoh Y, Nagase T, Arashi H, Yurimoto H, Miyagi I (1997) A new hydrous silicate, a water reservoir, in the upper part of the lower mantle. Geophys Res Lett 24: 1047–1050
Ohtani E, Kudoh Y, Naito H, Arashi H (1998) Stability of dense hydrous magnesium silicate phase G in the transition zone and the lower mantle. Mineral J 20: 163–169
Pacalo REG, Parise JB (1992) Crystal structure of superhydrous B, a hydrous magnesium silicate synthesized at 1400 °C and 20 GPa. Am Mineral 77: 681–684
Pawley AR, McMillan PF, Holloway JR (1993) Hydrogen in stishovite, with implications for mantle water content. Science 261: 1024–1026
Ringwood AE, Major A (1967) High-pressure reconnaissance investigations in the system Mg_2SiO_4-MgO-H_2O. Earth Planet Sci Lett 2: 130–133
Prewitt CT, Finger LW (1992) Crystal chemistry of high-pressure hydrous magnesium silicates. In: Syono Y, Manghnani MH (eds) High-pressure research in earth and planetary sciences. Am Geophys Union, Washington, DC, pp 269–274
Schreyer W (1995) Ultradeep metamorphic rocks: the retrospective viewpoint. J Geophys Res 100: B5, 8353–8366
Shieh SR, Mao HK, Ming JC (1998) Decomposition of phase D in the lower mantle and the fate of dense hydrous silicates in subducting slabs. Earth Planet Sci Lett 159: 13–23
Ulmer P, Trommsdorff V (1995) Serpentine stability to mantle depths and subduction-related magmatism. Science 268: 858–861
Yamamoto K, Akimoto S (1974) High-pressure and high-temperature investigations in the system MgO-SiO_2-H_2O. J Solid State Chem 9: 187–195
Yamamoto K, Akimoto S (1977) The system MgO-SiO_2-H_2O at high-pressures and high-temperatures – stability field for hydroxyl-clinohumite and 10-Å phase. Am J Sci 277: 288–312
Yang H, Prewitt CT, Frost DJ (1997) Crystal structure of the dense hydrous magnesium silicate, phase D. Am Mineral 82: 651–654
Yurimoto H, Kurosawa M, Sueno S (1989) Hydrogen analysis in quartz crystals and quartz glasses by secondary ion mass spectrometry. Geochim Cosmochim Acta 53: 751–755